Optimisation of an Ultrasonic Drill Horn for Planetary Sample Retrieval

Patrick Harkness
School of Engineering
University of Glasgow
Glasgow, United Kingdom
patrick.harkness@glasgow.ac.uk

Margaret Lucas
School of Engineering
University of Glasgow
Glasgow, United Kingdom
margaret.lucas@glasgow.ac.uk

***Abstract*—Ultrasonic tools can cut through foodstuffs, biological material and other soft matter with relative ease. However, when attempts are made to cut through harder material, the rate of progress markedly declines. Under such circumstances it is sometimes necessary to reduce the frequency of the blows delivered to the target, in order to ensure that each blow exceeds the compressive strength of the material, but for space applications the small size of high-frequency ultrasonic horns is extremely attractive. This paper therefore considers the optimization of horns for exploitation of the high-frequency/low-frequency drilling technique, whereby a free-mass oscillating between the horn and the target is employed to reduce the frequency at which impulse events are delivered to the target.**

Keywords-momentum exchange, frequency transformation; high-frequency/low-frequency drilling

I. INTRODUCTION

To learn about the history of other Earth-like worlds in the solar system, such as Mars, Europa and Titan, future planetary exploration missions will need the capability to drill into different surfaces to extract geological samples. Planetary drilling using traditional rotary tools is very difficult, as the low gravity and uncertain terrain makes reaction of drilling forces difficult. Even under close human supervision, rotary drill tools proved troublesome during the Apollo missions to the moon. [1]

Given that robotic exploration is likely to take place as a precursor to human exploration, the forces which can be reacted at the surface are likely to be further reduced because of the relative inflexibility of this platform and the time taken to react to commands from Earth. Therefore the low cutting forces and torques offered by ultrasonic tools are extremely attractive, especially because they obviate the need for a heavy drillstring structure.

The rate-of-progress of a percussive tool through rock is proportional to the effective impulse, which is impulse delivered above the specific compressive strength of the rock itself. [2] Ultrasonic horns, when applied directly to a rock, deliver their impulse at such a high frequency that a very low proportion of the impulse associated with each contact event is delivered above the compressive strength threshold. The technique of high-frequency/low-frequency drilling, where a free-mass oscillates between the tip of the ultrasonic horn and the target, effectively allows the energy supplied to the system to be delivered to the target at the lower oscillation frequency, as opposed to the higher ultrasonic frequency. Each contact event is therefore associated with increased impulse, and as the duration of the contact event is not significantly extended more of that impulse naturally must be delivered at a higher force, often exceeding the compressive strength threshold. The rate of progress is therefore increased.

The best performance will likely be derived from a horn which can cause the greatest acceleration of the free-mass during a contact event. It has been suggested [3] that dog-bone horns, which are a traditional step-horn with a flared tip to provide extra mass in the contact zone, are particularly well-suited to this application, but no optimization campaign has ever been undertaken. This work seeks to lay the foundation for such a campaign by analyzing the performance of a range of half-wavelength step-horns, tapered from a common base diameter to a range of tip diameters, in terms of the maximum change of velocity they can provide to a contacting free-mass.

II. THE RANGE OF HORNS

The step-horns are designed in the Abaqus finite-element (FE) package from 6/4 titanium alloy. The basal diameter is held at 34 mm, whilst the tip diameter (t_{tip}) is set to 10, 15, 20 and 25 mm. A fillet of diameter (34-t_{tip}) mm is provided at the step, and the length of the base and tip sections is set such that each is one-quarter wavelength when the horn is operating at a frequency (f) of 20 kHz (+/- 50 Hz) in the longitudinal mode. The horns are manufactured and examined by experimental modal analysis (EMA), with the data obtained by 3D laser vibrometry, and also by electrical impedance analysis (IA), being presented in Table I.

TABLE I. HORN PARAMETERS

t_{tip}	Longitudinal mode frequency and amplitude gain				
	f_{FE} (kHz)	f_{EMA} (kHz)	f_{IA} (kHz)	$Gain_{FE}$	$Gain_{EMA}$
10 mm	20.018	20.270	20.270	11.3	10.7
15 mm	20.029	20.169	20.180	5.0	4.7
20 mm	20.023	20.038	20.050	2.9	3.0
25 mm	19.992	19.944	19.970	1.9	1.8

III. Analytical Consideration of the Contact

A contact event between a free-mass and an ultrasonic horn can take place at any vibration phase angle, and it has been suggested [4] that both the phase angle on contact and the velocity of the incoming mass play a significant role in determining the change of velocity, or *"V*, delivered to the free-mass. The mass of the free-mass itself is set at 4 g, which is near the upper limit at which the oscillatory motion we seek can be excited. [5]

However it would be very difficult, in experiment, to time the impact event to a specific phase angle of a 20 kHz vibration. As this work seeks to compare the effect of horn geometries and not the effects of phase angle and incoming velocity, a slightly arbitrary condition is set for mathematical analysis – namely that the free-mass appears, with zero velocity, at the neutral point of the vibration locus just after the tip of the horn has withdrawn. The collision event subsequently occurs as the tip sweeps through on the forward stroke. Experimental results, described later in this paper, will be compared to this baseline.

An analytic model of the interaction between the tip of an ultrasonic horn and a free-mass can be approached as a simple momentum-exchange scenario, provided the mass and velocity of the tip are known. However an ultrasonic horn is not a rigid body with a single velocity, but rather behaves as a deforming body with no single unifying velocity. Secondly, the mass of the tip of the horn is an imprecise concept, as the tip itself must be rigorously defined.

This suggests the concept of the effective mass, which is that part of the tip involved in the collision event itself. The extent of the effective mass is defined by the volume swept by the shock generated at first contact before the contact event itself comes to an end. This is reasonable because no material outside this shock front can be considered to play a part in the dynamics of the collision.

In the first instance, a typical collision event is estimated to persist for one-quarter of a vibration cycle, which in this case is $^{1}/_{80,000}{}^{th}$ part of a second. Given the speed of sound in titanium alloy, 5,090 m/s, the depth of the effective mass may be approximately 6.4 cm and the mass involved may be evaluated by a trivial calculation. As this is the maximum extent of the effective mass, a value reduced by 50% (namely 3.2 cm) is used in the actual calculations to provide a realistic time-averaged value.

The velocity of the effective mass must also be calculated. Assuming a basal excitation of 5µm, the data in Table I can be used to yield the displacement at the very tip using the principles of simple harmonic motion. Although the average velocity of the effective mass section will be somewhat lower, as the velocity profile of a step-horn rises from zero at the nodal point to a maximum at the tip, it seems reasonable to use the value for velocity at the tip, namely the point of contact, because this will govern the actual interaction.

Under these circumstances and assumptions, the relevant equations governing the exchange of momentum during a collision event are given below, for simultaneous solution.

$$m_{eff}\,u_{bc} + m_{fr}\,v_{bc} = m_{eff}\,u_{ac} + m_{fr}\,v_{ac} \quad (1)$$

$$m_{eff}\,u_{bc}^2 + m_{fr}\,v_{bc}^2 = m_{eff}\,u_{ac}^2 + m_{fr}\,v_{ac}^2 \quad (2)$$

Here m_{eff} is the effective mass which is considered to have velocity u, m_{fr} is the free mass which has velocity v, and the scripts $_{bc}$ and $_{ac}$ refer to before collision and after collision, respectively.

IV. Numerical Consideration of the Contact

The numerical model of the contact event seeks to replicate the analytical examination, with the free-mass appearing at the neutral point just before the tip of the horn sweeps through that position. This is achieved by exciting a model of the transducer/horn/free-mass stack with a voltage signal applied across modeled piezoceramic elements in the transducer and phased such that the tip first retreats from the free-mass, leaving it momentarily hanging in free space with zero velocity, before sweeping back through and delivering the *"V* in question.

This approach is more complex than the analytical approach, as the contact event occurs within the start-up transient of the modelled ultrasonic system. In order to estimate a steady-state amplitude equivalent to the instantaneous transient amplitude at contact, the velocity at the moment of contact is used to yield an equivalent amplitude through the principles of simple harmonic motion. The model is then scaled to the 5µm baseline previously established.

Figures 1 – 4 show a collision event involving a horn with t_{tip} = 12.5 mm from just before first contact (Fig. 1) to just after separation (Fig. 4). Fig. 5 shows the position history of the tip of the horn and the free-mass before, during, and after this sequence.

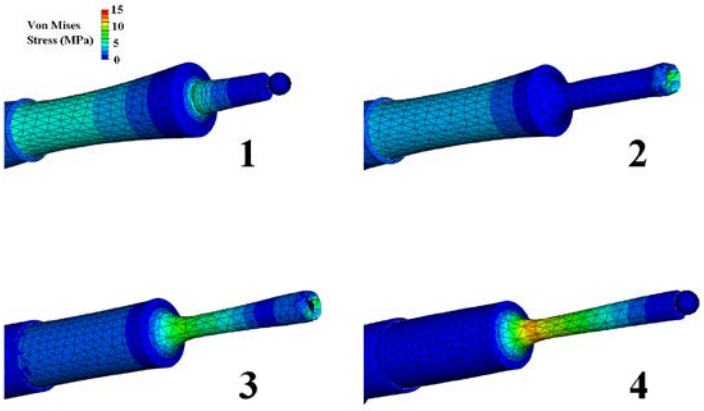

Figures 1 – 4. A contact event between a horn of t_{tip} = 12.5 mm and a free-mass, with exaggerated mechanical deformation and Von Mises stress contours, as evaluated in the time domain by Simulia Abaqus as part of the numerical consideration of the contact event. The frames 1 – 4 are respectively 0.065 ms, 0.069 ms, 0.073 ms and 0.077 ms after the voltage is applied, as a 20 kHz sine wave, to the piezoceramic elements (not shown).

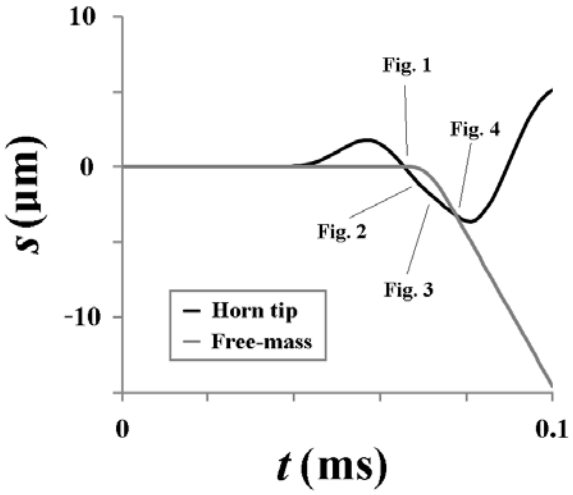

Figure 5. Position histories of the tip of the horn and the free-mass described in Figures 1 – 4. The locations of Figs. 1 – 4 are indicated, illustrating that the estimated contact duration of $^{1}/_{80,000}{}^{th}$ of a second is broadly accurate.

V. Experimental Consideration of the Contact

Due to the high speed of vibration, a simple experimental investigation of horn/free-mass interactions cannot guarantee the phase angle of contact, which as noted above is critical to the $"V$ imparted. However by arranging the horn vertically, with the free-mass inside a transparent tube to prevent horizontal movement, the $"V$ of an impact event can easily be determined by review of high-speed camera footage. To account for the uncertainty of phase angle, fifteen consecutive bounces of the free-mass are recorded.

On some occasions the outgoing speed of the free-mass is observed to be less than the incoming speed, but the reverse is usually true. This is entirely consistent with predictions made in the literature, which suggest that energy will usually be imparted to the free-mass. In this case, however, air resistance inside the tube prevents the bounces from growing ever-higher as the energy is imparted. Fig. 6 illustrates a typical frame from the high-speed camera, with the scale being used to determine the position of the free-mass (measuring to the reflection on the surface of the sphere) and the frame counter being used to determine time. Assuming g to be 9.8 m/s and losses due to air resistance to be negligible over the few tens of mm at the bottom of the tube, the incoming and outgoing speeds can be calculated from two known positions and times both just before and just after the contact event.

Each horn is turn is excited by a 5µm vibration at the base and the free-mass dropped onto the tip, through the tube, from a height of 1 m. Calculating $"V$ upon each of the subsequent fifteen encounters with each horn, where an increase of speed is interpreted as a positive $"V$ and a reduction in speed interpreted as negative, yields Table II. This table indicates that positive and negative $"V$ events are randomly distributed and that positive events outnumber the negative ones by 35 to 25, although this preponderance is not statistically significant over 60 events.

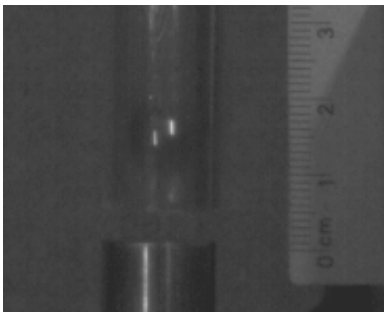

Figure 6. A still from the high-speed camera, showing a 4 g free-mass just above a horn of t_{tip} = 15 mm. The frame rate is 1,000 fps.

TABLE II. Magnitude of Recorded $"V Events

Bounce number	$"V (m/s) at different values of t_{tip}			
	10 mm	15 mm	20 mm	25 mm
1	-1.21	+1.11	+0.14	+0.34
2	-0.33	+1.76	+0.28	-0.76
3	+1.04	+0.07	+0.13	+0.17
4	-0.68	+0.72	-0.12	+0.71
5	+2.08	+1.11	-0.22	-0.36
6	-0.92	+0.93	-1.02	-0.27
7	-0.80	+0.89	-0.32	+0.52
8	+1.22	+1.23	+0.01	-0.08
9	+0.27	+0.47	-0.07	+0.28
10	+0.21	+1.4	+0.58	+0.56
11	-0.24	-1.95	+0.22	-0.27
12	+2.70	-0.15	+0.41	-0.56
13	+1.71	-0.20	-0.17	+0.28
14	-1.54	+0.60	-0.27	+0.30
15	-0.91	-0.55	+0.79	+0.41

Plotting the $"V$ events as a scatterplot, in Fig. 7, indicates that the largest changes of velocity are associated with the most tapered horns. As this work seeks to investigate the effect of horn geometry and not phase angle, the largest $"V$ events are selected and replotted in Fig. 8, which also shows the results of the earlier analytical and numerical analyses. It is apparent that there is agreement across the different procedures.

VI. Validation of the Results in Rock

The results suggest that, within the range of step-horns considered, low values of t_{tip} yield the most significant $"V$. When applied to the technique of high-frequency/low-frequency drilling these horns may therefore be expected to deliver the most effective impulse per unit time and per base excitation vibration amplitude, and therefore represent an attractive geometry for consideration. However, this is true only if the high stresses associated with highly-tapered step-horns can be accommodated or avoided.

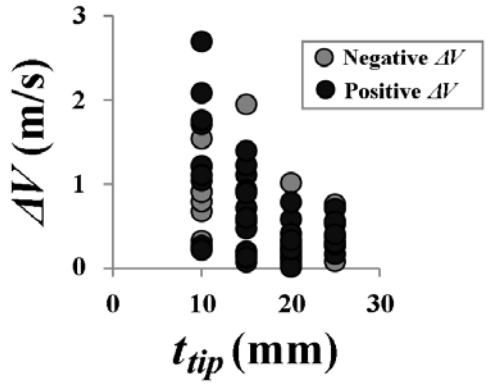

Figure 7. The recorded ” V on 15 consecutive bounces of a 4 g free-mass.

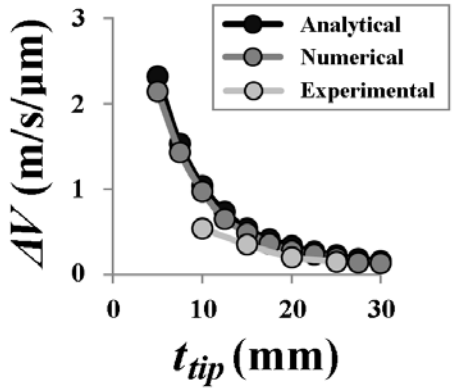

Figure 8. The largest recorded ” V compared to the analytical and numerical results, normalised per micron of base excitation vibration amplitude.

The hypothesis that increased *”V* will result in increased rock penetration can be demonstrated by testing the performance of the horns in a drilling experiment. Using the 5 μm base excitation previously adopted, which in experiment requires 25 W of power to maintain, a 4 g free-mass is used to drive a toothed titanium coring bit of diameter 38 mm (frontal area 170 mm^2) into Sherwood sandstone using each of the four step-horns in turn under a preload of 12 N. After a series of 5 minute drill runs using each horn at a new location, the sandstone test article is left as shown in Fig. 9. The drill sites, clockwise from top left, are created using horns with t_{tip} = 25 mm, 15 mm, 20 mm and 10 mm respectively. Periodic rotation of the bits is carried out to prevent tooth imprintation, which is known to slow progress by reducing the localized applied stress.

Measuring the depth of the excavation at each drill site at four circumferential points and then averaging the result yields the progress detailed in Table III.

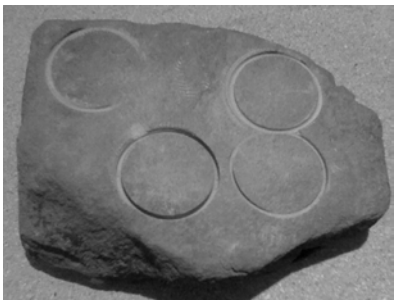

Figure 9. A sample of sandstone after being drilled by coring bits excited by the same free-mass, which is in turn powered by ultrasonic horns with the same base vibration amplitude. However, the effect of differing t_{tip} amongst the horns leads to differing rates-of-progress.

TABLE III. RATES OF PROGRESS

Progress over 5 minutes at different values of t_{tip}			
10 mm	**15 mm**	**20 mm**	**25 mm**
5	3.3	2	1.1

There is a correlation between t_{tip} and the rate-of-progress in sandstone which is consistent with increased *”V* capability yielding an increase in effective impulse.

VII. CONCLUSION

Several analyses suggest that highly-tapered ultrasonic horns are most effective for the transfer of momentum from the horn itself into a free-mass placed at the tip. Furthermore, increased acceleration of the free-mass is found to be associated with improved drilling performance.

These findings suggest that highly-tapered horns are indicated for high-frequency/low-frequency drill tools, provided that the stress concentrations associated with high-gain ultrasonic devices can be overcome.

REFERENCES

[1] R. Scheuring, J. Jones, J. Novak, J. Polk, D. Gillis, J. Schmid, J. Duncan, and J. Davis, “The Apollo Medical Operations Project: Recommendations to improve crew health and performance for future exploration missions and lunar surface operations,” *Acta Astronautica*, 2008, **63**, pp. 980-987.

[2] Z. Chang, S. Sherrit, X. Bao, and Y. Bar-Cohen, “Design and Analysis of Ultrasonic Horn for USDC (Ultrasonic/Sonic Driller/Corer),” *SPIE Smart Structures Conference*, San Diego, USA, 2004. Paper 5388-34.

[3] Y. Bar-Cohen, S. Sherrit, X. Bao, M. Badescu, J. Aldrich, and Z. Chang. “Subsurface Sampler and Sensors Platform Using the Ultrasonic/Sonic Driller/Corer (USDC),” *SPIE Smart Structures and Materials Symposium*, San Diego, USA, 2007. Paper 6529-18.

[4] X. Bao, Z. Chang, B. Dolgin, S. Sherrit, D. Pal, S. Du, and T. Peterson. “Modeling and Computer Simulation of Ultrasonic/Sonic Driller/Corer (USDC),” *IEEE Transactions on Ultrasonics, Ferroelectrics and Frequency Control*, 2003, **50**, 1147-1160.

[5] P. Harkness, A. Cardoni, M. Lucas and L. Waugh, “Optimization of the Horn, Free-Mass and Support Architecture of an Ultrasonic Rock-Boring System,” *AIAA Space 2010*, Anaheim, USA, 2010. AIAA 2010-8765.